IEEE Access
Multidisciplinary | Rapid Review | Open Access Journal

Received June 23, 2020, accepted July 1, 2020, date of publication July 9, 2020, date of current version July 22, 2020.

Digital Object Identifier 10.1109/ACCESS.2020.3008169

Novel Fixed-Time Nonsingular Fast Terminal Sliding Mode Control for Second-Order Uncertain Systems Based on Adaptive Disturbance Observer

HUIHUI PAN[1,2], GUANGMING ZHANG[1], HUIMIN OUYANG[1], (Senior Member, IEEE), AND LEI MEI[1], (Member, IEEE)

[1]School of Mechanical and Power Engineering, Nanjing Tech University, Nanjing 211816, China
[2]College of Electrical Engineering, Tongling University, Tongling 244061, China

Corresponding author: Guangming Zhang (zhgmnjtech@163.com)

This work was supported in part by the National Natural Science Foundation of China under Grant 61703202, and in part by the Key Research Development Project of Jiangsu Province under Grant BE2017164.

ABSTRACT In this paper, a novel fixed-time nonsingular fast terminal sliding mode control incorporating with an adaptive disturbance observer is proposed for second-order uncertain nonlinear systems to achieve fast stabilization and robust control. Based on the theory of fixed-time convergence, a novel fixed-time stable system is first investigated. Using this system, a novel fixed-time nonsingular fast terminal sliding mode controller is developed, which can achieve system stabilization within bounded convergence time regardless of initial states and provide nonsingularity and fast convergence. Moreover, an adaptive disturbance observer is designed to improve the control performance and compensate for uncertain disturbances. The fixed-time stability of the sliding surface and the system states under the proposed composite control scheme are demonstrated by the Lyapunov stability theory. Both theoretical analysis and simulation results are presented to verify the feasibility and superiority of the proposed method.

INDEX TERMS Nonsingular fast terminal sliding mode, adaptive disturbance observer, fixed-time stability.

I. INTRODUCTION

Sliding mode control (SMC) is a popular nonlinear control method thanks to its low insensitivity and strong robustness to system uncertainties [1]–[6], because many physical systems may suffer from various uncertainties [7], [8], such as parameter perturbation and external disturbance. In order to improve the convergence performance of conventional SMC, terminal sliding mode control (TSMC) has been proposed by using a nonlinear sliding hyperplane [9]–[12], which can achieve a fast finite-time convergence property in the sliding phase. Nevertheless, standard TSMC may occur a singularity problem. There are some modified terminal sliding surfaces presented for nonlinear systems to deal with the singularity problem, see, e.g., [9], [13]–[15].

It is worth noting that finite-time TSMC can force the system states to converge to equilibrium within bounded time related to initial states, which prohibits its application into practical systems if the initial conditions are unknown in prior. As an extension of finite-time stability theory, the fixed-time stability theory was given in [16]. Compared to the finite-time stability, the fixed-time stability can provide the desirable convergence within bounded time without requiring the knowledge of initial conditions. Because of the good feature, fixed-time TSMC has been studied extensively in recent years. The literature [17] developed a fast fixed-time nonsingular TSMC scheme which was used to suppress chaos in power systems. The literature [18] constructed a new nonsingular fast terminal sliding surface that was employed to the fixed-time tracking control for second-order multi-agent systems. In [19], a novel fixed-time nonsingular TSMC method was proposed, which was applied to intercept maneuvering targets. The literature [20] presented a novel nonsingular terminal sliding mode manifold for the fixed-time robust stabilization of second-order nonlinear uncertain systems. Fixed-time terminal sliding surfaces were designed for the tracking control of the rigid spacecraft [21]–[23]. The literature [24] proposed a novel fixed-time nonsingular TSMC strategy that was used to control a single inverted pendulum.

The associate editor coordinating the review of this manuscript and approving it for publication was Shihong Ding.

As known,TSMC is a robust control algorithm which can suppress uncertain disturbances. Nevertheless, the robust performance is closely related to the chattering frequency of the controller. It means that large robust switching gains are designed, which in turn may result in aggravation of the undesired chattering.If the disturbances can be compensated accurately, then the chattering can be substantially reduced while guaranteeing the robustness of the system [25]–[27]. Recently, the researches on the disturbance observer-based methods have received considerable attention. In [28], a novel terminal sliding mode tracking control method was presented utilizing disturbance observer technique for uncertain SISO nonlinear systems. In [29], a novel sliding surface was constructed based on disturbance estimation for disturbance suppression. The literature [30] proposed a novel composite controller by using continuous TSMC method and disturbance observer technique where the bounds of disturbance derivatives were assumed to be known. In [31], a composite controller was developed by integrating finite-time control method and finite-time disturbance observer technique for a class of disturbed system.The literature [32] proposed a disturbance observer-based integral SMC strategy for singularly perturbed systems with mismatched disturbances. An improved SMC method using disturbance observer was presented to control a permanent magnet synchronous motor [33]. The literature [34] used an adaptive nonsingular TSMC incorporating with a nonlinear disturbance observer to control a nonlinear mass-spring damper system, where the observer error converged to a small region near zero. In these methods, the disturbance is estimated by a disturbance observer, and it is fed back to the control law to compensate for its influence. Moreover, the disturbance observer can be employed to reduce chattering in sliding mode control.

Motivated by the above discussions, this paper is devoted to propose a novel composite control scheme for second-order uncertain nonlinear systems to achieve fast fixed-time convergence and reduce chattering. The proposed control method has advantages in convergence rate and chattering reduction over the existing results of fixed-time stable control methods. The main contributions of this paper are summarized as follows:

1. A novel fixed-time stable system is investigated.Using this system, a novel fixed-time nonsingular fast terminal sliding mode manifold is designed, which can guarantee the fixed-time system stabilization regardless of initial states. The singularity problem is avoided by introducing a new nonlinear piecewise function.

2. A novel adaptive disturbance observer is developed, which can achieve fast exact lumped disturbance estimation in finite time and do not require information about the bounds on the disturbances and their derivatives.

3. A novel composite control scheme is proposed by integrating a novel fixed-time nonsingular fast terminal sliding mode controller and a novel adaptive disturbance observer. The proposed method is not only robust to uncertain disturbances, but also can achieve fast fixed-time convergence of the system.

This paper is organized as follows. Section II provides some useful lemmas. In Section III, a novel composite controller is developed for second-order uncertain nonlinear systems. Simulation results illustrate the feasibility and superiority of the proposed control method in Section IV. Section V is the conclusion.

Throughout the whole paper, $\mathrm{sig}(x)^{\alpha}$ denotes $|x|^{\alpha}\,\mathrm{sign}(x)$.

II. MATHEMATICAL PRELIMINARIES

Considering a second-order system with disturbance, given by:

$$\begin{cases} \dot{x}_1 = x_2 \\ \dot{x}_2 = F(x) + B(x)u + D \end{cases} \tag{1}$$

where x_1 and x_2 are system states. $F(x)$ and $B(x)$ are smooth nonlinear functions of x, u is the control input, and D is the disturbance.

Definition 1 [35]: Consider the following dynamic system:

$$\dot{x}(t) = f(x(t)), x(0) = x_0 \tag{2}$$

where $x \in R^n, f(x) : D \in R^n$ is a continuous nonlinear function that is on open neighborhood $D \subseteq R^n$ of the origin, and $f(0) = 0$. The origin is regarded as a fixed-time stable equilibrium point if it is finite-time stable with bounded convergence time function $T(x_0)$, i.e., there exists $T_{\max} > 0$ such that $T(x_0) < T_{\max}$.

Lemma 1 [36]: Consider a scalar system:

$$\dot{y} = -\alpha \mathrm{sig}(y)^{\psi} - \beta \mathrm{sig}(y)^{\varphi} \tag{3}$$

where $\alpha > 0, \beta > 0, \psi > 1, 0 < \varphi < 1$. The system (3) is fixed-time stable, and the convergence time T is bounded by:

$$T < \frac{1}{\alpha(\psi - 1)} + \frac{1}{\beta(1 - \varphi)} \tag{4}$$

Lemma 2 [24]: Consider the following differential equation:

$$\dot{y} = -\alpha \mathrm{sig}(y)^{\kappa} - \beta \mathrm{sig}(y)^{\varphi} \tag{5}$$

where $\alpha > 0, \beta > 0, \kappa = 0.5(\psi + 1) + 0.5(\psi - 1)\mathrm{sign}(|y| - 1), \psi > 1, 0 < \varphi < 1$. The system (5) is fixed-time stable, and the convergence time T is bounded by:

$$T < \frac{1}{\alpha(\psi - 1)} + \frac{1}{\beta(1 - \varphi)} \ln(1 + \frac{\alpha}{\beta}) \tag{6}$$

Lemma 3: Consider the following differential equation:

$$\dot{y} = -\alpha \mathrm{sig}(y)^{\kappa} - \beta \mathrm{sig}(y)^{\gamma} \tag{7}$$

where $\alpha > 0, \beta > 0, \kappa = 0.5(\psi + 1) + 0.5(\psi - 1)\mathrm{sign}(|y| - 1), \gamma = 0.5(\psi + \varphi) + 0.5(\psi - \varphi)\mathrm{sign}(|y| - 1), \psi > 1, 0 < \varphi < 1$. The system (7) is fixed-time stable, and the convergence time T is bounded by:

$$T < \frac{1}{(\alpha + \beta)(\psi - 1)} + \frac{1}{\beta(1 - \varphi)} \ln(1 + \frac{\alpha}{\beta}) \tag{8}$$

Proof: The differential equation for the system (7) can be rewritten as:

$$\begin{cases} \dot{y} = -\alpha \mathrm{sig}(y)^{\psi} - \beta \mathrm{sig}(y)^{\psi}, & |y| > 1 \\ \dot{y} = -\alpha y - \beta \mathrm{sig}(y)^{\varphi}, & |y| \le 1 \end{cases} \tag{9}$$

By solving (9), the upper bound of convergence time can be calculated as:

$$\begin{aligned} T_{\max} &= \lim_{y(0)\to\infty} \Big(\int_{1}^{y(0)} \frac{1}{(\alpha+\beta)\,\mathrm{sig}(y)^{\psi}} dy \\ &\quad + \int_{0}^{1} \frac{1}{\alpha y + \beta \mathrm{sig}(y)^{\varphi}} dy \Big) \\ &= \lim_{y(0)\to\infty} \frac{1-|y(0)|^{1-\psi}}{(\alpha+\beta)(\psi-1)} + \frac{1}{\beta(1-\varphi)} \ln(1+\frac{\alpha}{\beta}) \\ &= \frac{1}{(\alpha+\beta)(\psi-1)} + \frac{1}{\beta(1-\varphi)} \ln(1+\frac{\alpha}{\beta}) \end{aligned} \tag{10}$$

The proof is completed.

Remark 1: Note that system (3) was investigated in [36]. System (5) was presented in [24], which is extended from (3) and has faster convergence than (3). However, the convergence time of system (5) is not an optimal one. In this paper, system (7) is proposed, which can achieve faster convergence in comparisons with (3) and (5).

III. THE COMPOSITE CONTROLLER DESIGN

A. NOVEL FIXED-TIME NONSINGULAR FAST TERMINAL SLIDING MODE

According to Lemma 3, a novel fixed-time terminal sliding surface can be constructed as:

$$s = x_2 + \alpha_1 \mathrm{sig}(x_1)^{\kappa_1} + \beta_1 \mathrm{sig}(x_1)^{\gamma_1} \tag{11}$$

where $\alpha_1 > 0, \beta_1 > 0, \kappa_1 = 0.5(\psi_1+1) + 0.5(\psi_1-1)\mathrm{sign}(|x_1|-1)$, $\gamma_1 = 0.5(\psi_1+\varphi_1) + 0.5(\psi_1-\varphi_1)\mathrm{sign}(|x_1|-1), \psi_1 > 1, 0 < \varphi_1 < 1$.

The time derivative of the sliding surface s defined by (11) can be obtained:

$$\dot{s} = \dot{x}_2 + \alpha_1\kappa_1 |x_1|^{\kappa_1-1} x_2 + \beta_1\gamma_1 |x_1|^{\gamma_1-1} x_2 \tag{12}$$

In (12), it can be easily observed that if $x_1 = 0$ and $x_2 \neq 0$, the singularity may occur due to $\varphi_1 - 1 < 0$.

In [37],to avoid singularity problem, a nonlinear function was presented as:

$$\omega_0(x_1) = \begin{cases} \mathrm{sig}(x_1)^{\varphi_1}, & |x_1| > \delta \\ \varpi_0 x_1 + \sigma_0 \mathrm{sig}(x_1)^2, & |x_1| \le \delta \end{cases} \tag{13}$$

where $0 < \delta < 1$, $\varpi_0 = (2-\varphi_1)\delta^{\varphi_1-1}$, $\sigma_0 = (\varphi_1-1)\delta^{\varphi_1-2}$.

To speed up the convergence rate in the region $x_1 \in [0, \delta]$, the following nonlinear function is introduced as:

$$\omega_1(x_1) = \begin{cases} \mathrm{sig}(x_1)^{\varphi_1}, & |x_1| > \delta \\ \varpi_1 \sin(x_1) + \sigma_1 \mathrm{sig}(x_1)^{\theta}, & |x_1| \le \delta \end{cases} \tag{14}$$

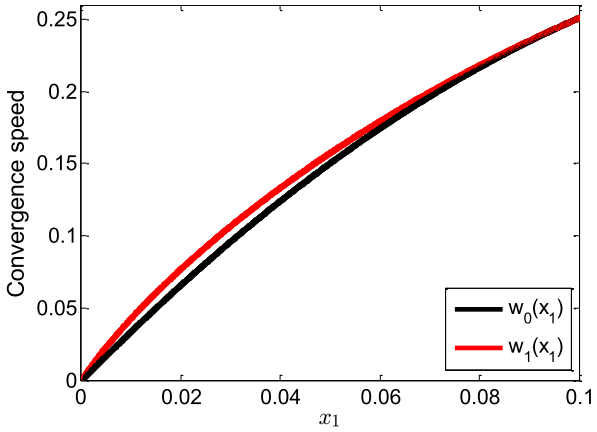

FIGURE 1. The comparison of convergence speed.

where $\varpi_1 = \frac{\varphi_1\delta^{\varphi_1} - \theta\delta^{\varphi_1}}{\delta\cos(\delta) - \theta\sin(\delta)}$, $\sigma_1 = \frac{\varphi_1\delta^{\varphi_1-1} - \varpi_1\cos(\delta)}{\theta\delta^{\theta-1}}$, $0 < \delta < 1, 1 < \theta < 2$. It is worth noticing that the nonlinear function is continuous and derivable.

The parameters in functions $\omega_0(x_1)$ and $\omega_1(x_1)$ are set as $\delta = 0.1, \varphi_1 = 0.6$, and $\theta = 1.2$. The convergence speed response curves of $\omega_0(x_1)$ and $\omega_1(x_1)$ in the region $x_1 \in [0, \delta]$ are illustrated in Fig.1. It can be seen clearly from Fig.1 that the function $\omega_1(x_1)$ has the faster convergence rate than $\omega_0(x_1)$.

Combining the nonlinear function, a novel fixed-time nonsingular fast terminal sliding mode manifold can be put forward as follows:

$$s = x_2 + \alpha_1 \mathrm{sig}(x_1)^{\kappa_1} + \beta_1 \omega(x_1) \tag{15}$$

with

$$\omega(x_1) = \begin{cases} \mathrm{sig}(x_1)^{\gamma_1}, & |x_1| > \delta \\ \varpi \sin(x_1) + \sigma \mathrm{sig}(x_1)^{\theta}, & |x_1| \le \delta \end{cases} \tag{16}$$

where $\varpi = \frac{\varphi_1\delta^{\varphi_1} - \theta\delta^{\varphi_1}}{\delta\cos(\delta) - \theta\sin(\delta)}$, $\sigma = \frac{\varphi_1\delta^{\varphi_1-1} - \varpi\cos(\delta)}{\theta\delta^{\theta-1}}$.

Eq.(15) is equivalent to the following form:

$$s = \begin{cases} x_2 + \alpha_1 \mathrm{sig}(x_1)^{\psi_1} + \beta_1 \mathrm{sig}(x_1)^{\psi_1}, & |x_1| > 1 \\ x_2 + \alpha_1 x_1 + \beta_1 \mathrm{sig}(x_1)^{\varphi_1}, & \delta < |x_1| \le 1 \\ x_2 + \alpha_1 x_1 + \beta_1(\varpi \sin(x_1) + \sigma \mathrm{sig}(x_1)^{\theta}), & |x_1| \le \delta \end{cases} \tag{17}$$

According to (17), the proposed sliding mode manifold is divided into three separate parts, which can achieve a fast convergence rate either far from or close to the equilibrium point. The singularity problem is avoided since the sliding mode manifold is switched into the general sliding mode manifold when x_1 enters into the region $|x_1| \le \delta$, as shown in Fig.2.

B. ADPTIVE DISTURBANCE OBSERVER

In practical application, it is usually difficult to require the prior information about the disturbance D. In this section, an adaptive disturbance observer is developed for system (1)

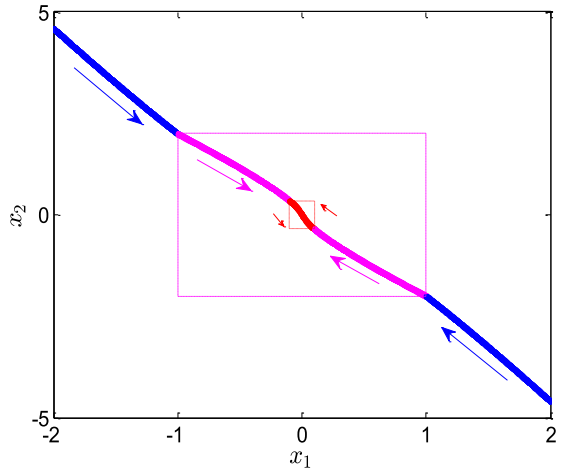

FIGURE 2. The proposed sliding surface on the phase plane.

to compensate the disturbance, so that the system control performance can be improved.

Assumption 1: The uncertain disturbance D in system (1) is continuous. The first and second derivatives of D exist as $|\dot{D}| < D_1$, $|\ddot{D}| < D_2$,where upper bound D_1 and D_2 are unknown positive constants.

To estimate the disturbance for system (1), a new form of adaptive disturbance observer is designed as:

$$\begin{cases} e = \phi - x_2 \\ \Lambda = \dot{e} + \alpha_3 \mathrm{sig}(e)^{\psi_3} + \beta_3 \mathrm{sig}(e)^{\varphi_3} \\ \dot{\phi} = F(x) + B(x)u + \hat{D} - \alpha_3 \mathrm{sig}(e)^{\psi_3} - \beta_3 \mathrm{sig}(e)^{\varphi_3} \\ \dot{\hat{D}} = -\alpha_4 \mathrm{sig}(\Lambda)^{\psi_4} - \beta_4 \mathrm{sig}(\Lambda)^{\varphi_4} - \upsilon(t)\mathrm{sign}(\Lambda) \end{cases} \tag{18}$$

where $\alpha_3, \beta_3, \alpha_4, \beta_4 > 0, \psi_3, \psi_4 > 1, 0 < \varphi_3, \varphi_4 < 1$, and $\upsilon(t)$ is an adaptive gain.

Theorem 1: Using the designed observer in (18), when the condition $\upsilon(t) > |\dot{D}|$ is satisfied in finite time, then the disturbance estimation error will converge to zero in finite time.

Proof: According to (18),the first derivative of e is given by:

$$\dot{e} = \dot{\phi} - \dot{x}_2 = \hat{D} - D - \alpha_3 \mathrm{sig}(e)^{\psi_3} - \beta_3 \mathrm{sig}(e)^{\varphi_3} \tag{19}$$

Substituting (19) into (18),one can obtain $\Lambda = \hat{D} - D$, then the time derivative of Λ is

$$\begin{aligned} \dot{\Lambda} &= \dot{\hat{D}} - \dot{D} \\ &= -\alpha_4 \mathrm{sig}(\Lambda)^{\psi_4} - \beta_4 \mathrm{sig}(\Lambda)^{\varphi_4} - \upsilon(t)\mathrm{sign}(\Lambda) - \dot{D} \end{aligned} \tag{20}$$

Consider the Lyapunov function $V_1 = 0.5\Lambda^2$, then its time derivative is

$$\begin{aligned} \dot{V}_1 &= \Lambda\dot{\Lambda} \\ &= -\alpha_4 |\Lambda|^{\psi_4+1} - \beta_4 |\Lambda|^{\varphi_4+1} - \upsilon(t)|\Lambda| - \dot{D}\Lambda \\ &\le -\alpha_4 |\Lambda|^{\psi_4+1} - \beta_4 |\Lambda|^{\varphi_4+1} - (\upsilon(t) - |\dot{D}|)|\Lambda| \end{aligned} \tag{21}$$

Since the condition $\upsilon(t) > |\dot{D}|$ is achieved in finite time, it is concluded that $\dot{V}_1 \le 0$.Then, the sliding mode manifold Λ can converge to zero in finite time, i.e. $\Lambda = 0$. Define the disturbance estimation error $e_D = \hat{D} - D$, it is concluded that $e_D = \Lambda = 0$. Thus, the proposed observer can estimate the disturbance accurately in finite time.

The proof is completed.

Next, the objective is to construct adaptive algorithm for $\upsilon(t)$ to satisfy the condition $\upsilon(t) > |\dot{D}|$. Motivated by the research work in [38], $\upsilon(t)$ is given by the following two layers adaptive law:

$$\begin{cases} \dot{\upsilon}(t) = -(\upsilon_0 + \upsilon_1(t))\mathrm{sign}(\varepsilon) \\ \dot{\upsilon}_1(t) = \begin{cases} \upsilon_d |\varepsilon|, |\varepsilon| > \varepsilon_0 \\ 0, |\varepsilon| \le \varepsilon_0 \end{cases} \end{cases} \tag{22}$$

with

$$\varepsilon = \upsilon(t) - \frac{|\chi|}{\eta_0} - \eta_1 \tag{23}$$

$$\dot{\chi} = \lambda fal(-\upsilon(t)\mathrm{sign}(\Lambda) - \chi, \mu, \delta_0) \tag{24}$$

$$fal(a, \mu, \delta_0) = \begin{cases} \mathrm{sig}(a)^{\mu}, & |a| > \delta_0 \\ \dfrac{a}{\delta_0^{1-\mu}}, & |a| \le \delta_0 \end{cases} \tag{25}$$

where $\upsilon_0, \upsilon_d, \lambda > 0, 0 < \eta_0, \eta_1, \mu, \delta_0 < 1$.

Remark 2: Note that, a $fal(\cdot)$ function filter not only has good filtering effect, but also has fast tracking performance. A close approximation of $-\upsilon(t)\mathrm{sign}(\Lambda)$ can be obtained in real-time by the $fal(\cdot)$ function filter.

Proposition 1: $\eta_0, \eta_1, \varepsilon_0, \tau$, and υ_d are designed so that the following inequalities:

$$\frac{|\chi|}{\eta_0} + \frac{\eta_1}{2} > |D_1| \tag{26}$$

$$\varepsilon_0^2 + \frac{\tau^2 D_1^2}{\upsilon_d \eta_0^2} < \frac{\eta_1^2}{4} \tag{27}$$

hold for any given D_1, then the condition $\upsilon(t) > |\dot{D}|$ can be achieved in finite time.

Proof: To facilitate analysis, denote

$$\zeta = \frac{\tau D_1}{\eta_0} - \upsilon_1(t) \tag{28}$$

where $\tau > 1$, and τ is designed to ensure $\tau \ge |\dot{\chi}|/D_1$.

To analyze the variables ε and ζ, choosing a Lyapunov function $V_2 = 0.5\varepsilon^2 + 0.5\zeta^2/\upsilon_d$, its time derivative is

$$\begin{aligned} \dot{V}_2 &= \varepsilon\dot{\varepsilon} + \frac{1}{\upsilon_d}\zeta\dot{\zeta} \\ &= \varepsilon\left(-(\upsilon_0 + \upsilon_1(t))\mathrm{sign}(\varepsilon) - \frac{|\dot{\chi}|}{\eta_0}\right) + \frac{1}{\upsilon_d}\zeta\dot{\zeta} \\ &\le -(\upsilon_0 + \upsilon_1(t))|\varepsilon| + \frac{|\dot{\chi}|}{\eta_0}|\varepsilon| + \frac{1}{\upsilon_d}\zeta\dot{\zeta} \end{aligned} \tag{29}$$

Case I: If $|\varepsilon| > \varepsilon_0$, according to (28) and (29), it can be obtained

$$\begin{aligned} \dot{V}_2 &\le -\upsilon_0|\varepsilon| - \upsilon_1(t)|\varepsilon| + \frac{|\dot{\chi}|}{\eta_0}|\varepsilon| - \left(\frac{\tau D_1}{\eta_0} - \upsilon_1(t)\right)|\varepsilon| \\ &\le -\upsilon_0|\varepsilon| \end{aligned} \tag{30}$$

Case II: If $|\varepsilon| \leq \varepsilon_0$ and $\zeta < 0$, then $\varepsilon\dot{\varepsilon} \leq -\upsilon_0 |\varepsilon| + \zeta |\varepsilon| \leq 0$,and

$$\dot{V}_2 \leq -\upsilon_0 |\varepsilon| + \zeta |\varepsilon| - \zeta |\varepsilon| \leq -\upsilon_0 |\varepsilon| \tag{31}$$

Case III: If $|\varepsilon| \leq \varepsilon_0$ and $\zeta \geq 0$, because $\dot{\upsilon}_1(t) > 0$, then $\zeta \leq \tau D_1/\eta_0$ for all time. It follows that $\dot{V}_2 < 0$, outside of the region $\Omega = \{(\varepsilon, \zeta) : |\varepsilon| \leq \varepsilon_0, 0 \leq \zeta < \tau D_1/\eta_0\}$. Define a small region $V_0 = \{(\varepsilon, \zeta) : V < 0.5\varepsilon_0^2 + 0.5(\tau D_1/\eta_0)^2/\upsilon_d\}$, it encloses the region Ω. Choose appropriate parameters to ensure that (27) can be satisfied. When (ε, ζ) enters V_0 as case III, then (ε, ζ) can not leave V_0 because V_0 is a fixed region. According to (27), $|\varepsilon| < \eta_1/2$.

Yet as case I and II, (ε, ζ) does not enter V_0, and $\dot{V}_2 < 0$. According to Barbalat's Lemma, it can be concluded that ε can converge to zero asymptotically [38]. It implies that there exists a finite time t_0 such that $|\varepsilon| < \eta_1/2$ for $t > t_0$.

Therefore, whether (ε, ζ) enters V_0 or not, the inequality $|\varepsilon| < \eta_1/2$ is satisfied in finite time. Then,

$$|\varepsilon(t)| = \left|\upsilon(t) - \frac{|\chi|}{\eta_0} - \eta_1\right| < \frac{\eta_1}{2} \tag{32}$$

So

$$\upsilon(t) - \frac{|\chi|}{\eta_0} - \eta_1 > -\frac{\eta_1}{2} \tag{33}$$

and the condition in (26) is satisfied, then

$$\upsilon(t) > \frac{|\chi|}{\eta_0} + \frac{\eta_1}{2} > |D_1| \tag{34}$$

According to Assumption 1, $|\dot{D}| < D_1$, then the condition $\upsilon(t) > \dot{D}$ can be achieved in finite time.

The proof is completed.

C. CONTROL LAW DESIGN

According to (1), (15), and (16), the time derivative of the proposed sliding surface can be given by:

$$\dot{s} = F(x) + B(x)u + D + \alpha_1\kappa_1 |x_1|^{\kappa_1 - 1} x_2 + \beta_1\dot{\omega}(x_1)x_2 \tag{35}$$

with

$$\dot{\omega}(x_1) = \begin{cases} \gamma_1 |x_1|^{\gamma_1 - 1} x_2, & |x_1| > \delta \\ \varpi \cos(x_1)x_2 + \sigma\theta |x_1|^{\theta - 1} x_2, & |x_1| \leq \delta \end{cases} \tag{36}$$

To ensure the system trajectory fast reach the designed sliding surface from any initial conditions, a novel fixed-time reaching law can be designed as:

$$\dot{s} = -\alpha_2 \mathrm{sig}(s)^{\kappa_2} - \beta_2 \mathrm{sig}(s)^{\gamma_2} \tag{37}$$

where $\alpha_2 > 0, \beta_2 > 0, \kappa_2 = 0.5(\psi_2 + 1) + 0.5(\psi_2 - 1)\mathrm{sign}(|s| - 1), \gamma_2 = 0.5(\psi_2 + \varphi_2) + 0.5(\psi_2 - \varphi_2)\mathrm{sign}(|s| - 1), \psi_2 > 1, 0 < \varphi_2 < 1$.

Based on the output of the observer in (18), substituting (35) into (37), a novel fixed-time nonsingular fast terminal sliding mode control based on an adaptive disturbance observer (NFNTSMC-ADO) is designed as:

$$u = -\frac{1}{B(x)}(F(x) + \hat{D} + \alpha_1\kappa_1 |x_1|^{\kappa_1 - 1} x_2 + \beta_1\dot{\omega}(x_1)x_2 + \alpha_2 \mathrm{sig}(s)^{\kappa_2} + \beta_2 \mathrm{sig}(s)^{\gamma_2}) \tag{38}$$

D. STABILITY ANALYSIS

Theorem 2: Consider the system (1), applying the control law in (38), the designed sliding surface s can converge to zero in fixed time, and the system states will converge to a small region $R = \{(x_1, x_2) : |x_1| \leq \delta, |x_2| \leq \alpha_1\delta + \beta_1\delta^{\varphi_1}\}$ in fixed time.

Proof: Substituting (38) into (35), $\dot{s}$ can be given by:

$$\dot{s} = -\alpha_2 \mathrm{sig}(s)^{\kappa_2} - \beta_2 \mathrm{sig}(s)^{\gamma_2} - \hat{D} + D \tag{39}$$

Consider a Lyapunov function $V_3 = s^2$, the time derivative of V_3 can be given by:

$$\begin{aligned} \dot{V}_3 &= 2s\dot{s} \\ &= -2s(\alpha_2 \mathrm{sig}(s)^{\kappa_2} + \beta_2 \mathrm{sig}(s)^{\gamma_2} + \hat{D} - D) \\ &= -2\alpha_2 |s|^{\kappa_2 + 1} - 2\beta_2 |s|^{\gamma_2 + 1} - 2e_D s \end{aligned} \tag{40}$$

According to Theorem 1, the disturbance estimation error can converge to zero in finite time. It means that there exists a finite time T^* such that $e_D = 0$ for $t > T^*$. Define the reaching time of the sliding surface as T_r. Choose appropriate values for $\alpha_2, \beta_2, \psi_2, \varphi_2$, and observer parameters to satisfy the condition $T_r > T^*$, then,

$$\begin{aligned} \dot{V}_3 &= -2\alpha_2 |s|^{\kappa_2 + 1} - 2\beta_2 |s|^{\gamma_2 + 1} \\ &= -2\alpha_2 V_1^{\frac{\kappa_2 + 1}{2}} - 2\beta_2 V_1^{\frac{\gamma_2 + 1}{2}} \end{aligned} \tag{41}$$

According to Lemma 3,the sliding surface can be reached in fixed time, and the upper bound of convergence time can be given by:

$$T_r < \frac{1}{(\alpha_2 + \beta_2)(\psi_2 - 1)} + \frac{1}{\beta_2(1 - \varphi_2)} \ln(1 + \frac{\alpha_2}{\beta_2}) \tag{42}$$

When $s = 0$, the stability analysis of the system states convergence to the region near zero is given as follows:

Case I: If $|x_1| > \delta$, from (15), the following equation can be obtained:

$$s = x_2 + \alpha_1 \mathrm{sig}(x_1)^{\kappa_1} + \beta_1 \mathrm{sig}(x_1)^{\gamma_1} = 0 \tag{43}$$

Consider a candidate Lyaunov function $V_4 = x_1^2$, then the time derivative of V_4 can be given by:

$$\begin{aligned} \dot{V}_4 &= 2x_1\dot{x}_1 \\ &= 2x_1(-\alpha_1 \mathrm{sig}(x_1)^{\kappa_1} - \beta_1 \mathrm{sig}(x_1)^{\gamma_1}) \\ &= -2\alpha_1 V_2^{\frac{\kappa_1 + 1}{2}} - 2\beta_1 V_2^{\frac{\gamma_1 + 1}{2}} \end{aligned} \tag{44}$$

According to Lemma 3 and (44), it is concluded that the system state x_1 will converge to the region $|x_1| \leq \delta$ and the convergence time T_s is bounded by:

$$T_s < \frac{1}{(\alpha_1 + \beta_1)(\psi_1 - 1)} + \frac{1}{\beta_1(1 - \varphi_1)} \ln(1 + \frac{\alpha_1}{\beta_1}) \tag{45}$$

Moreover, from (43), it can be obtained:

$$|x_2| \leq \alpha_1 |x_1| + \beta_1 |x_1|^{\varphi_1} \leq \alpha_1\delta + \beta_1\delta^{\varphi_1} \tag{46}$$

Therefore, the system state x_2 can converge to the region $|x_2| \leq \alpha_1\delta + \beta_1\delta^{\varphi_1}$ in fixed time. The convergence time for the system (1) can be calculated as:

$$T = T_r + T_s < \frac{1}{(\alpha_2+\beta_2)(\psi_2-1)} + \frac{1}{\beta_2(1-\varphi_2)}\ln(1+\frac{\alpha_2}{\beta_2}) + \frac{1}{(\alpha_1+\beta_1)(\psi_1-1)} + \frac{1}{\beta_1(1-\varphi_1)}\ln(1+\frac{\alpha_1}{\beta_1}) \quad (47)$$

Case II: If $|x_1| \leq \delta$, it means that the system state x_1 has converged to the region $|x_1| \leq \delta$ in fixed time. Applying (15), (48) can be obtained:

$$s = x_2 + \alpha_1 x_1 + \beta_1(\varpi \sin(x_1) + \sigma \mathrm{sig}(x_1)^{\theta}) \quad (48)$$

From (48), the following inequality can be obtained:

$$\begin{aligned} |x_2| &\leq \alpha_1 |x_1| + \beta_1(\varpi |\sin(x_1)| + \sigma |x_1|^{\theta}) \\ &\leq \alpha_1\delta + \beta_1\delta^{\varphi_1} \end{aligned} \quad (49)$$

Thus, according to (49),the system states will converge to the finite set $R = \{(x_1, x_2) : |x_1| \leq \delta, |x_2| \leq \alpha_1\delta + \beta_1\delta^{\varphi_1}\}$ in fixed time.

The proof is completed.

Remark 3: The disturbance is quickly estimated by the designed observer in (18). Moreover, the disturbance is eliminated quickly under the control law in (38), then the sliding surface and the system states can converge to their desired values in fixed time.

Remark 4: Note that, using the proposed sliding surface in (15), the system states can not strictly converge to zero, which means that small steady-state errors may be brought. By designing appropriate parameters, the steady-state errors can be small enough, which may not affect the convergence accuracy of the system.

IV. SIMULATION RESULTS

In this section, the proposed composite control scheme is applied to a Van der Pol circuit system and a two-link rigid robotic manipulator system. Simulation results confirm the effectiveness and superiority of the proposed method.

A. VAN DER POL CICUITS SYSTEM

Consider the Van der Pol circuit system, as follows [28]:

$$\begin{cases} \dot{x}_1 = x_2 \\ \dot{x}_2 = -2x_1 + 3x_2(1-x_1^2) + u + d \end{cases} \quad (50)$$

According to (18), the adaptive disturbance observer is designed as:

$$\begin{cases} e = \phi - x_2 \\ \Lambda = \dot{e} + \alpha_3 \mathrm{sig}(e)^{\psi_3} + \beta_3 \mathrm{sig}(e)^{\varphi_3} \\ \dot{\phi} = -2x_1 + 3x_2(1-x_1^2) + u + \hat{d} - \alpha_3 \mathrm{sig}(e)^{\psi_3} \\ \qquad -\beta_3 \mathrm{sig}(e)^{\varphi_3} \\ \dot{\hat{d}} = -\alpha_4 \mathrm{sig}(\Lambda)^{\psi_4} - \beta_4 \mathrm{sig}(\Lambda)^{\varphi_4} - \upsilon(t)\mathrm{sign}(\Lambda) \end{cases} \quad (51)$$

in which $\upsilon(t)$ is updated by the adaptive law in (22).

Next, according to the NFNTSMC-ADO technique, the new fixed-time nonsingular sliding mode manifold and the control law are constructed as:

$$s = \dot{x}_1 + \alpha_1 \mathrm{sig}(x_1)^{\kappa_1} + \beta_1 \omega(x_1) \quad (52)$$

$$u = 2x_1 - 3x_2(1-x_1^2) - \hat{d} - \alpha_1\kappa_1 |x_1|^{\kappa_1 - 1} x_2 - \beta_1 \dot{\omega}(x_1)x_2 - \alpha_2 \mathrm{sig}(s)^{\kappa_2} - \beta_2 \mathrm{sig}(s)^{\gamma_2} \quad (53)$$

The initial conditions for the system and the disturbance observer are assumed as $x_1(0) = 2, x_2(0) = -1$, and $\hat{d}(0) = 0$, respectively. The controller and observer parameters are set as $\alpha_1 = \beta_1 = \alpha_3 = \beta_3 = 2, \alpha_2 = \beta_2 = \psi_3 = 3, \varphi_1 = \varphi_2 = 0.6, \psi_1 = \psi_2 = \psi_4 = 2, \alpha_4 = \beta_4 = 6, \varphi_3 = \varphi_4 = 0.5$, $\upsilon_0 = 0.1, \delta = \delta_0 = 0.01, \eta_0 = 0.999, \eta_1 = 0.65, \lambda = 60$, and $\mu = 0.9$.

In the first simulation test, the disturbance is assumed as $d = 0$. For comparison, a novel fixed-time nonsingular fast terminal sliding mode controller (NFNTSMC), a modified fixed-time nonsingular fast terminal sliding mode controller (FNTSMC) proposed in [19] and a conventional fixed-time nonsingular fast terminal sliding mode controller (NTSMC) proposed in [14] are designed as follows:

NFNTSMC:

$$s = \dot{x}_1 + \alpha_1 \mathrm{sig}(x_1)^{\kappa_1} + \beta_1 \omega(x_1) \quad (54)$$

$$u = 2x_1 - 3x_2(1-x_1^2) - \alpha_1\kappa_1 |x_1|^{\kappa_1 - 1} x_2 - \beta_1 \dot{\omega}(x_1)x_2 - \alpha_2 \mathrm{sig}(s)^{\kappa_2} - \beta_2 \mathrm{sig}(s)^{\gamma_2} \quad (55)$$

FNTSMC:

$$s = \dot{x}_1 + \alpha_1 \mathrm{sig}(x_1)^{\kappa_1} + \beta_1 \omega_0(x_1) \quad (56)$$

$$u = 2x_1 - 3x_2(1-x_1^2) - \alpha_1\kappa_1 |x_1|^{\kappa_1 - 1} x_2 - \beta_1 \dot{\omega}_0(x_1)x_2 - \alpha_2 \mathrm{sig}(s)^{\kappa_2} - \beta_2 \mathrm{sig}(s)^{\varphi_2} \quad (57)$$

NTSMC:

$$s = \dot{x}_1 + \alpha_1 \mathrm{sig}(x_1)^{\psi_1} + \beta_1 \omega_0(x_1) \quad (58)$$

$$u = 2x_1 - 3x_2(1-x_1^2) - \alpha_1\psi_1 |x_1|^{\psi_1 - 1} x_2 - \beta_1 \dot{\omega}_0(x_1)x_2 - \alpha_2 \mathrm{sig}(s)^{\psi_2} - \beta_2 \mathrm{sig}(s)^{\varphi_2} \quad (59)$$

Three controllers are employed to stabilize system (50). The results given in Fig.3 illustrate that the system states are steered to their desired values, respectively. Compared with FNTSMC and NTSMC, NFNTSMC takes shorter time for the reaching motion. Moreover, NFNTSMC makes the system states x_1 and x_2 converge to equilibrium more quickly than FNTSMC and NTSMC. Comparative results show that NFNTSMC has better control performance than two other controllers with respect to faster convergence speed and shorter reaching time.

In the second simulation test, the disturbance is assumed as $d = 3\sin(0.5\pi t) + 0.5\sin(2\pi t)$.The response curves of the system variables under NFNTSMC-ADO and NFNTSMC are shown in Figs.4-6.

The disturbance and its estimation are displayed in Fig.4. It is clear to see that the proposed disturbance observer can estimate the disturbance in finite time. Fig.5 shows that the

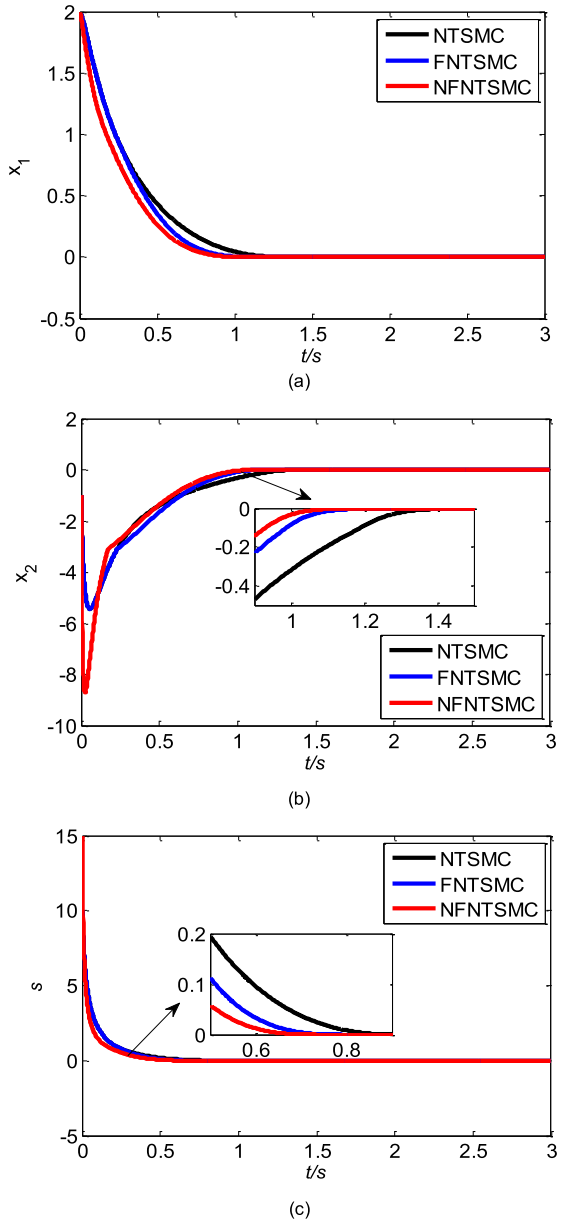

FIGURE 3. The response curves of state variables (a)x_1.(b) x_2.(c)s.

adaptive gain $\upsilon(t)$ dynamically changes according to $\left|\dot{d}\right|$. Moreover, it can be observed that the condition $\upsilon(t) > \left|\dot{d}\right|$ is achieved in finite time. Based on Theorem 1, the stability of the proposed disturbance observer can be guaranteed. The simulation results in Fig.4 agree with Theorem 1.

As shown in Fig.6, it can be noted that the disturbance compensation is able to affect the convergence rate to some extent. Furthermore, it is obvious that NFNTSMC-ADO can substantially reduce the chattering of the system states and the sliding surface in comparison with NFNTSMC. That is because NFNTSMC-ADO utilizes an adaptive disturbance observer to accurately estimate the disturbance and compensate the disturbance online. These simulation results confirm that the proposed NFNTSMC-ADO method can be employed

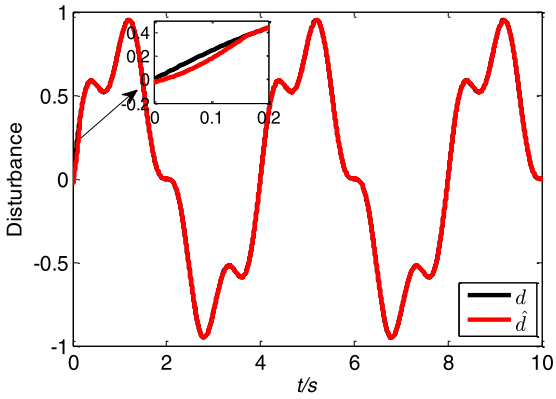

FIGURE 4. Disturbance and its estimation.

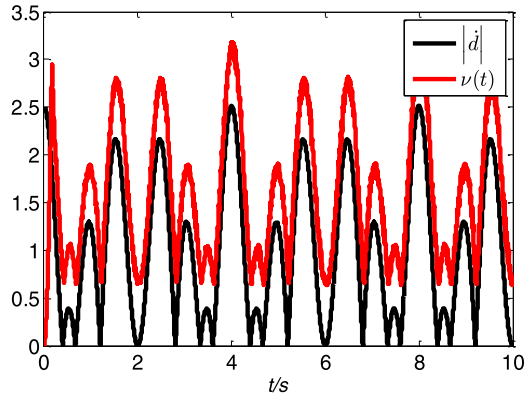

FIGURE 5. The curves of $\left|\dot{d}\right|$ and $\upsilon(t)$.

to improve the dynamic performance and stability of the system.

In the third simulation test for verifying the fixed-time convergence of the proposed composite controller, other three different initial states are set as: 1) $[x_1, x_2] = [2.5, -0.5]$, 2) $[x_1, x_2] = [5, -2]$, 3)$[x_1, x_2] = [8, -1]$. The design parameters of NFNTSMC-ADO are consistent with above. Based on Theorem 2, the upper bound of convergence time for the sliding surface and the system states are calculated as 0.74s and 1.86s, respectively. It is obvious from Fig.7 that the sliding surface and the system states can converge to their equilibrium within bounded convergence time. Moreover, the simulation results confirm that the time taken to reach the desired values of system states from different initial states under uncertain disturbance is guaranteed to be fixed time, and the upper bound convergence time of the system is only related to the design parameters.

To conclude, NFNTSMC has a faster convergence rate than FNTSMC and NTSMC. NFNTSMC-ADO has higher accuracy control and lower chattering in comparison with NFNTSMC. Furthermore, NFNTSMC-ADO can achieve fast fixed-time convergence. Thus, it can be seen that the proposed composite control scheme can achieve promising control performance.

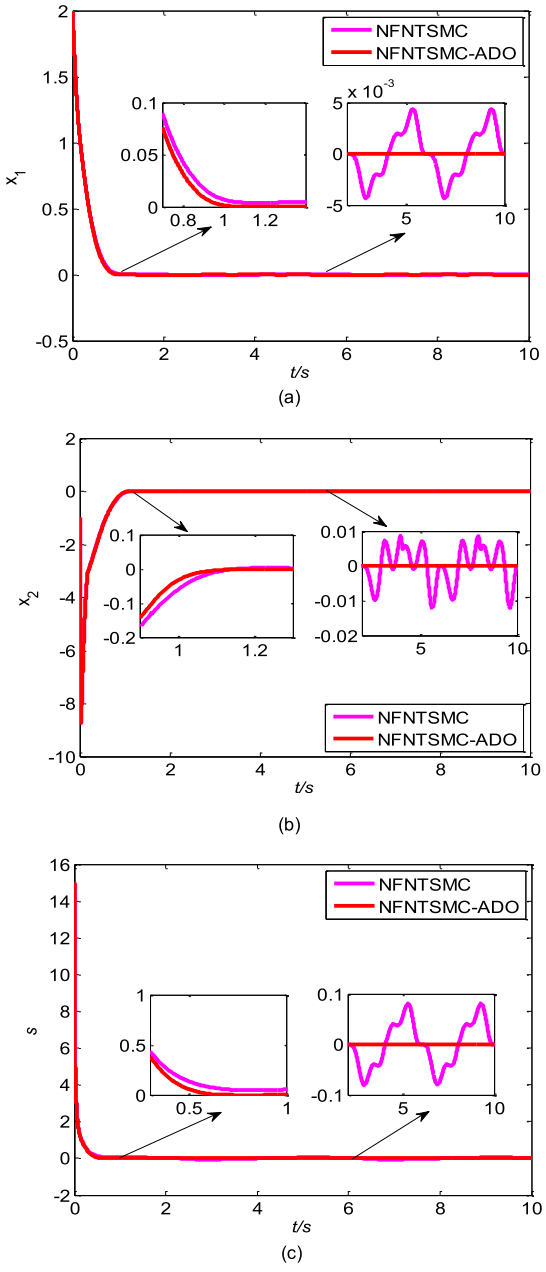

FIGURE 6. The response curves of state variables (a) x_1. (b) x_2.(c)s.

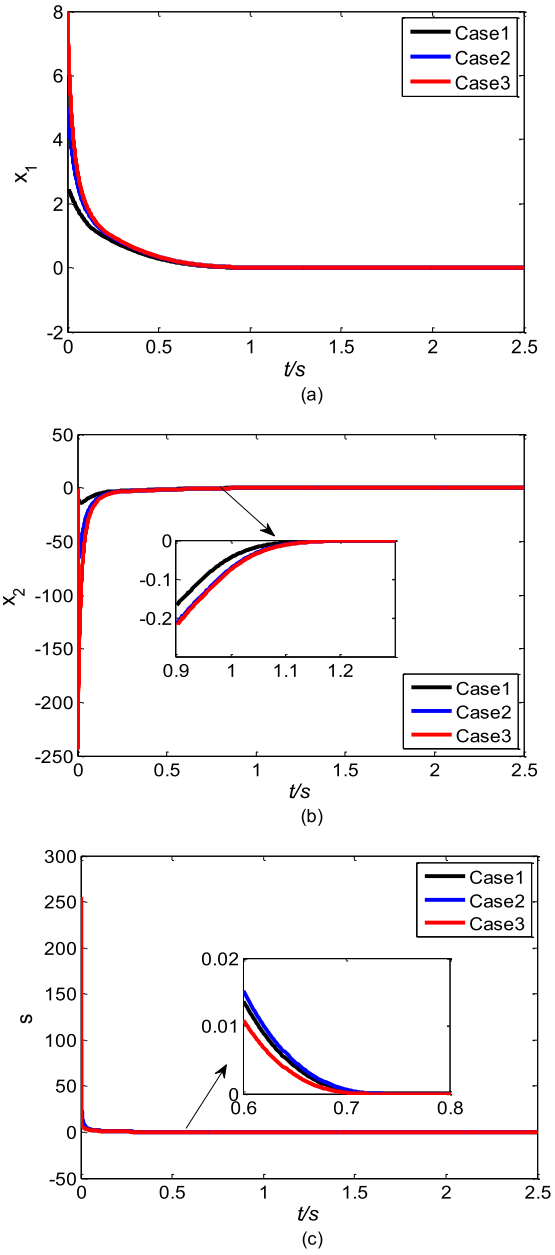

FIGURE 7. The response curves of state variables(a) x_1. (b) x_2. (c) s.

B. TWO-LINK RIGID ROBOT MANIPULATOR

As in [39],the dynamic equation of a two-link manipulator model can be described as:

$$M(q)\ddot{q} + C(q,\dot{q})\dot{q} + G(q) = u + d \tag{60}$$

in which, the involved matrices can be given by:

$$M(q) = \begin{bmatrix} (m_1+m_2)l_1^2+m_2l_2^2 & m_2l_2^2 + m_2l_1l_2\cos(q_2) \\ +2m_2l_1l_2\cos(q_2)+J_1 & \\ m_2l_2^2+m_2l_1l_2\cos(q_2) & m_2l_2^2 + J_2 \end{bmatrix},$$

$$C(q,\dot{q}) = \begin{bmatrix} -m_2l_1l_2\sin(q_2)\dot{q}_1 & -2m_2l_1l_2\sin(q_2)\dot{q}_1 \\ 0 & m_2l_1l_2\sin(q_2)\dot{q}_2 \end{bmatrix},$$

$$G(q) = \begin{bmatrix} (m_1+m_2)gl_1\cos(q_2) + m_2gl_2\cos(q_1+q_2) \\ m_2gl_2\cos(q_1+q_2) \end{bmatrix}.$$

where q_i, $\dot{q}_i$, and $\ddot{q}_i$ denote the vectors of joint position, velocity and acceleration, respectively. m_i is the link mass, J_i is the link moment of inertia given in the centre of mass. u and d represent the torque input and the uncertain disturbance, respectively.

The system parameters are set as $m_1 = 0.5\text{kg}, m_2 = 1.5\text{kg}, l_1 = 1\text{m}, l_2 = 0.8\text{m}, J_1 = 5\text{kg}\cdot\text{m}^2, J_2 = 5\text{kg}\cdot\text{m}^2, g = 9.8\text{N/s}^2, q(0) = [1.2, 0.8]^T, \dot{q}(0) = [0, 0]^T$. The

desired signals are given by $q_d = [q_{1d}, q_{2d}]^T$ with $q_{1d} = 0.35e^{-4t} - 1.4e^{-t} + 1.25$ and $q_{2d} = e^{-t} - 0.25e^{-4t} + 1.25$.

Denote $x = [x_1, x_2]^T = [q, \dot{q}]^T$, (60) can be rewritten as:

$$\begin{cases} \dot{x}_1 = x_2 \\ \dot{x}_2 = f(x) + b(x)u + D \end{cases} \tag{61}$$

where $f(x) = -M_0^{-1}(x_1)(C_0(x)x_2 + G_0(x_1))$, $b(x) = M_0^{-1}(x_1)$, $D = -M_0^{-1}(x_1)(\Delta M(x_1)\dot{x}_2 + \Delta C(x)x_2 + \Delta G(x_1) - d)$. In which, $M_0(x_1)$, $C_0(x)$, $G_0(x_1)$ are nominal values, and $\Delta M(x_1)$, $\Delta C(x)$, $\Delta G(x_1)$ are uncertain terms.

According to (18), the adaptive disturbance observer is designed as:

$$\begin{cases} e = \phi - x_2 \\ \Lambda = \dot{e} + \alpha_3 \mathrm{sig}(e)^{\psi_3} + \beta_3 \mathrm{sig}(e)^{\varphi_3} \\ \dot{\phi} = f(x) + b(x)u + \hat{D} - \alpha_3 \mathrm{sig}(e)^{\psi_3} - \beta_3 \mathrm{sig}(e)^{\varphi_3} \\ \dot{\hat{D}} = -\alpha_4 \mathrm{sig}(\Lambda)^{\psi_4} - \beta_4 \mathrm{sig}(\Lambda)^{\varphi_4} - \upsilon(t)\mathrm{sign}(\Lambda) \end{cases} \tag{62}$$

in which $\upsilon(t) = [\upsilon_1(t), \upsilon_2(t)]$, and they are updated by the adaptive law in (22).

Denote $x_d = [x_{1d}, x_{2d}]^T = [q_d, \dot{q}_d]^T$, define $\xi_1 = q - q_d$, $\xi_2 = \dot{q} - \dot{q}_d$, then the error equation of the rigid robotic manipulator can be obtained:

$$\begin{cases} \dot{\xi}_1 = \xi_2 \\ \dot{\xi}_2 = F(\xi) + B(\xi)u + D \end{cases} \tag{63}$$

where $F(\xi) = f(x) - \ddot{q}_d$, $B(\xi) = M_0^{-1}(x_1)$.

Based on the strategy of NFNTSMC-ADO, the fixed-time nonsingular terminal sliding surface and the control law are designed as:

$$s = \xi_2 + \alpha_1 \mathrm{sig}(\xi_1)^{\kappa_1} + \beta_1 \omega(\xi_1) \tag{64}$$

$$\begin{aligned} u = -B^{-1}(\xi)(F(\xi) + \hat{D} + \alpha_1\kappa_1 |\xi_1|^{\kappa_1 - 1}\xi_2 \\ + \beta_1 \dot{\omega}(\xi_1)\xi_2 + \alpha_2 \mathrm{sig}(s)^{\kappa_2} + \beta_2 \mathrm{sig}(s)^{\gamma_2}) \end{aligned} \tag{65}$$

where $s = [s_1, s_2]^T$, $\mathrm{sig}(\xi_1)^{\kappa_1} = [\mathrm{sig}(\xi_{11})^{\kappa_{11}}, \mathrm{sig}(\xi_{12})^{\kappa_{12}}]^T$, $\omega(\xi_1) = [\omega(\xi_{11}), \omega(\xi_{12})]^T$, $\mathrm{sig}(s)^{\kappa_2} = [\mathrm{sig}(s_1)^{\kappa_{21}}, \mathrm{sig}(s_2)^{\kappa_{22}}]^T$, $\mathrm{sig}(s)^{\gamma_2} = [\mathrm{sig}(s_1)^{\gamma_{21}}, \mathrm{sig}(s_2)^{\gamma_{22}}]^T$.

The controller and disturbance parameters are chosen as $\alpha_1 = \beta_1 = diag\{1.5, 1.5\}$, $\psi_1 = 3$, $\psi_2 = \psi_3 = 2$, $\psi_4 = 1.5$, $\alpha_2 = \beta_2 = diag\{2, 2\}$, $\alpha_3 = \beta_3 = diag\{1, 1\}$, $\alpha_4 = \beta_4 = diag\{7, 1\}$, $\varphi_1 = \varphi_2 = \varphi_3 = \varphi_4 = 0.6$, $\theta = 1.5$, $\delta = \delta_0 = 0.01$, $\upsilon_0 = 0.1$, $\eta_0 = 0.999$, $\eta_1 = 0.6$, $\mu = 0.9$, and $\lambda = diag\{15, 15\}$.

In the first simulation test, the external disturbances are set as $d = [0, 0]^T$. Three controllers, NFNTSMC, FNTSMC and NTSMC, are designed by reference to the above example for the purpose of comparison.

The position tracking responses of joints 1,2 using the three controllers are depicted in Fig.8. Fig.9 shows the time responses of tracking errors obtained by utilizing the three controllers.It is concluded from Figs.8-9 that in comparison with the two other controllers, the system states track the desired signals more quickly under NFNTSMC. The time responses of the sliding surfaces are plotted in Fig.10. It can

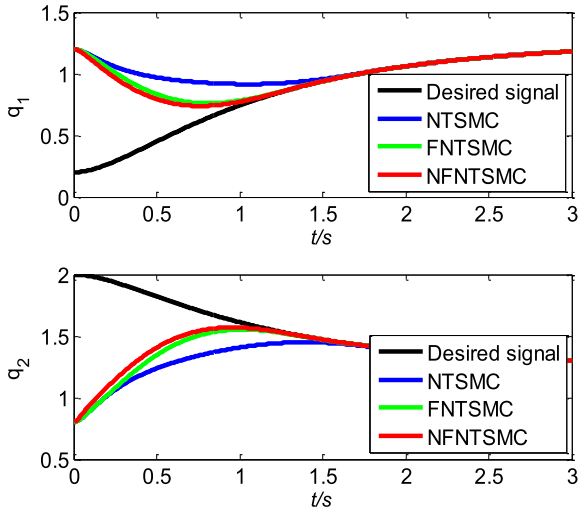

FIGURE 8. The tracking performances of joints 1 and 2.

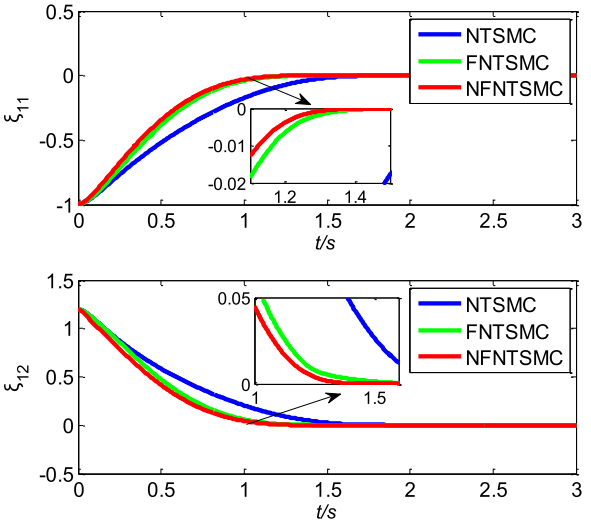

FIGURE 9. The tracking errors of joints 1 and 2.

be obviously observed from Fig.10 that the tracking errors reach the desgined sliding surfaces with less time under NFNTSMC compared to FNTSMC and NTSMC. Therefore, NFNTSMC has the faster convergence rate than FNTSMC and NTSMC.

In the second simulation test, the disturbance is assumed as $d = [5\cos(\pi t); 2\sin(\pi t)]$.Shown in Figs.11-14 are the time responses of the state variables under NFNTSMC-ADO and NFNTSMC. The disturbance and its estimation are plotted in Fig.11. It is seen from Fig.12 that the condition $\upsilon(t) > |\dot{d}|$ can be satisfied in finite time. According to Theorem 1, ADO can accurately estimate the disturbance in finite time. The simulation results in Fig.11 agree with Theorem 1. The tracking errors of joints 1 and 2 under the two control schemes are presented in Fig.13. Fig.14 shows the time responses of sliding surfaces obtained by the two control schemes. Compared with NFNTSMC, NFNTSMC-ADO can largely

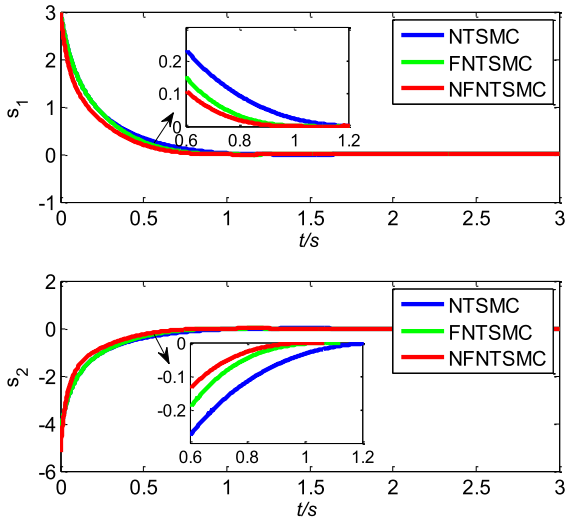

FIGURE 10. The sliding surfaces under the three controllers.

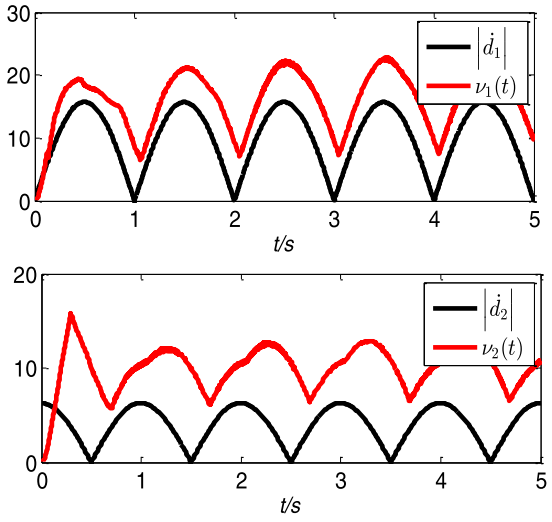

FIGURE 12. The curves of $|\dot{d}|$ and $v(t)$.

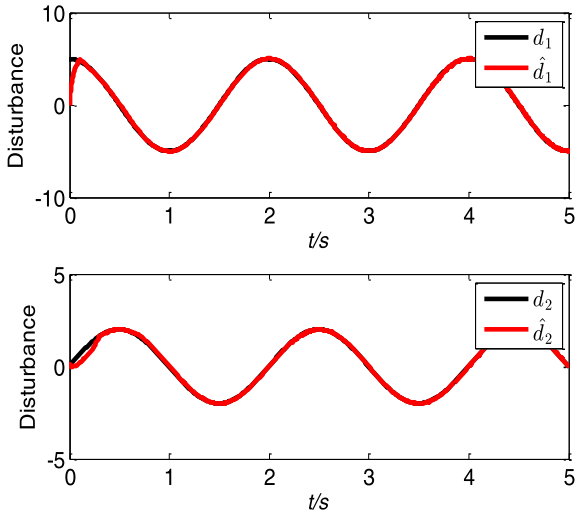

FIGURE 11. The disturbance and its estimation.

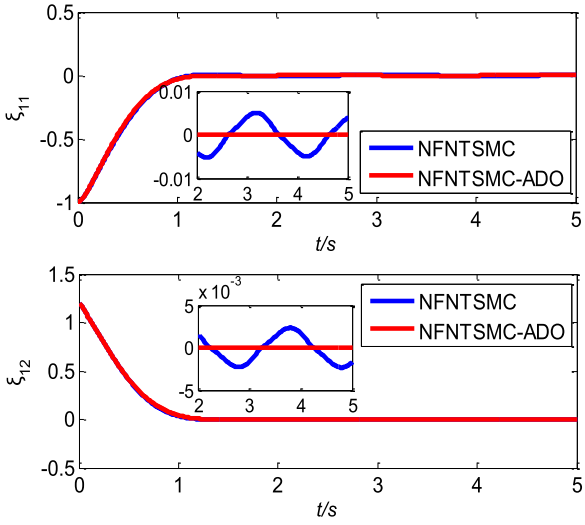

FIGURE 13. The tracking error of joints 1 and 2.

alleviate the chattering of system states and sliding surfaces because ADO can accurately estimate the disturbances which are utilized in the control law. Thus, NFNTSMC-ADO can achieve better tracking performance and higher precision than NFNTSMC.

In addition to external disturbances, considering the sudden load variation in the running robotic manipulators, it is assumed that the mass of joint 2 increases to 2.5kg after $t \geq 2$s. As shown in Figs.15-16, the fluctuation of the tracking errors and the sliding surfaces are small under NFNTSMC-ADO. Moreover, the recovery time of both the tracking errors and the sliding surfaces convergence to zero are short under NFNTSMC-ADO. Thus, it can be seen that the proposed NFNTSMC-ADO technique achieves good property of nominal performance recovery.

In a word, NFNTSMC-ADO exhibits the fine properties of disturbance rejection and strong robustness.

In the third simulation test, other three different initial states are set as: 1)$q = [2, 1]^T$, 2) $q = [5, 0.5]^T$, 3)$q = [10, 0]^T$. The parameters selection of NFNTSMC-ADO is consistent with above. According to Theorem 2, the upper bound time of the sliding surfaces convergence to zero is 1.12s, and the upper bound time of the system states reaching stabilization is 2.44s.

Figs.17-19 show the position tracking responses, tracking errors and sliding surfaces of joints 1 and 2 with different initial states under NFNTSMC-ADO, respectively. It is not difficult to find that the convergence time of the sliding surfaces and the system states do not exceed the calculated upper bound convergence time. It can be seen that the proposed NFNTSMC-ADO scheme can not only force the sliding surface to the equilibrium point in fixed time, but also drive system states to reach stabilization in fixed time. Simulation results given in Figs.17-19 verify the proposed composite

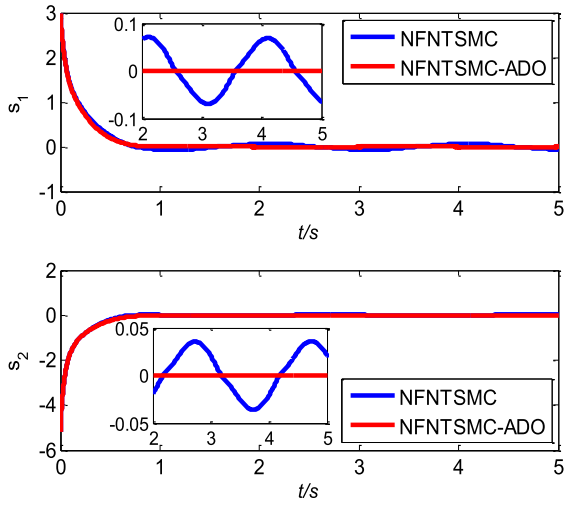

FIGURE 14. The sliding surfaces under the two control schemes.

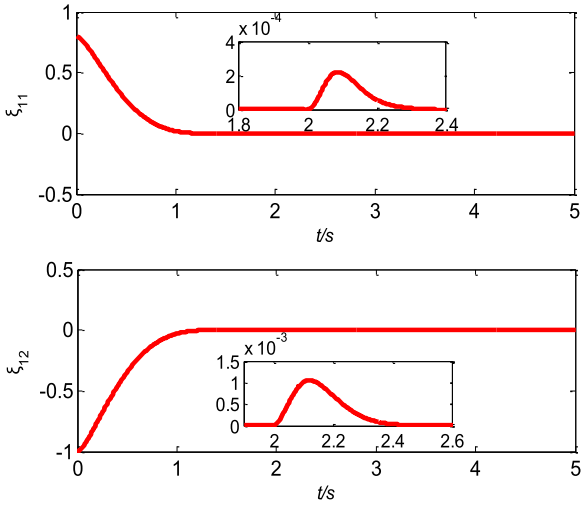

FIGURE 15. The tracking errors of joints 1 and 2 under NFNTSMC-ADO scheme.

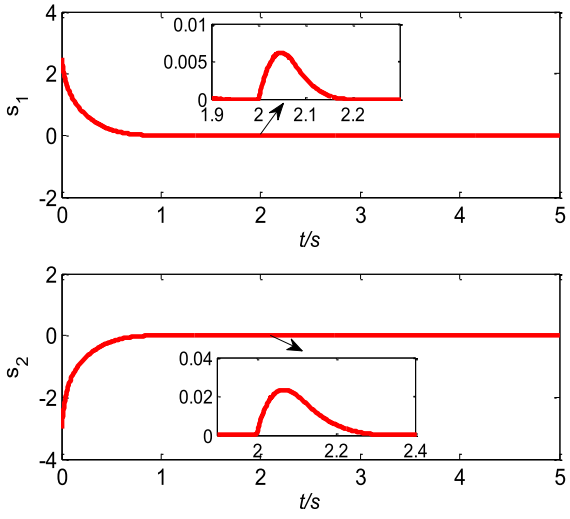

FIGURE 16. The sliding surfaces under NFNTSMC-ADO scheme.

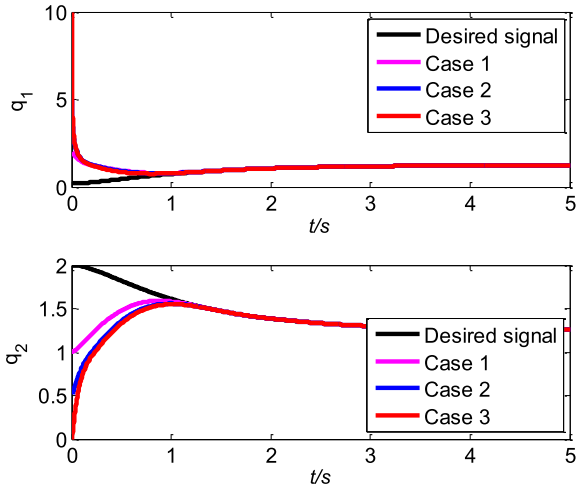

FIGURE 17. tracking performances of joints 1 and 2 with three cases.

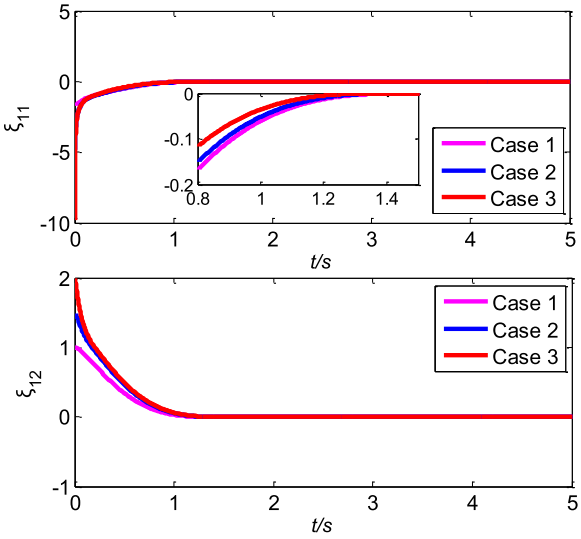

FIGURE 18. The tracking error of joints 1 and 2 with three cases.

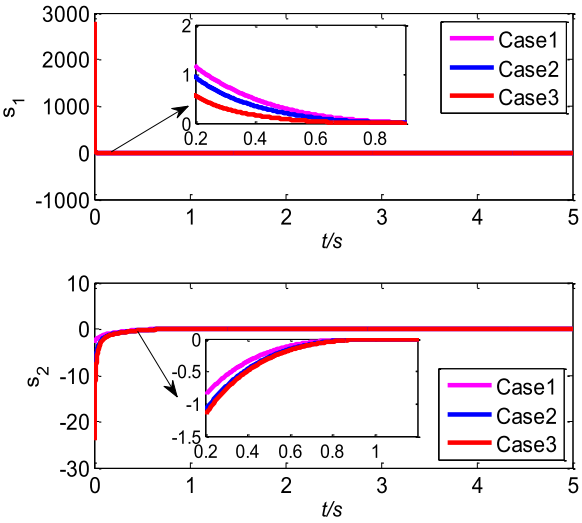

FIGURE 19. The sliding surfaces with three cases.

control technique can achieve the fixed-time convergence regardless of the initial states.

In summary, NFNTSMC has the faster convergence rate than FNTSMC and NTSMC. NFNTSMC-ADO has smaller

tracking errors and lower chattering in comparison with NFNTSMC. Furthermore, NFNTSMC-ADO can achieve system stabilization within fixed time. Therefore, it can be concluded that the proposed composite controller is a robust controller with fast fixed-time convergence and good tracking precision.

V. CONCLUSION

In this paper, an adaptive disturbance observer-based fixed-time nonsingular fast terminal sliding mode control method is investigated for second-order uncertain nonlinear systems. A novel fixed-time stable system is presented. Combining this system and a new nonlinear piecewise function, a novel fixed-time nonsingular fast terminal sliding mode controller is developed, which can force the system states to reach stabilization within fixed time. To reduce the influence of disturbance, an adaptive disturbance observer is designed to accurately estimate the disturbance that is fed back to the control law. Simulation results illustrate that the proposed composite control method can exhibit satisfactory control performance with fast convergence, high precision, and strong robustness. It is worthwhile noticing that the control method can be also applied to other complicated second-order uncertain systems.This method is extended to n-order systems with mismatched disturbance, which would be a future research work.

REFERENCES

[1] H. Li, P. Shi, and D. Yao, "Adaptive sliding-mode control of Markov jump nonlinear systems with actuator faults," *IEEE Trans. Autom. Control*, vol. 62, no. 4, pp. 1933–1939, Apr. 2017.

[2] S. Ding, L. Liu, and W. X. Zheng, "Sliding mode direct yaw-moment control design for in-wheel electric vehicles," *IEEE Trans. Ind. Electron.*, vol. 64, no. 8, pp. 6752–6762, Aug. 2017.

[3] Y. Han, Y. Cheng, and G. Xu, "Trajectory tracking control of AGV based on sliding mode control with the improved reaching law," *IEEE Access*, vol. 7, pp. 20748–20755, 2019.

[4] H. Ouyang, J. Wang, G. Zhang, L. Mei, and X. Deng, "Novel adaptive hierarchical sliding mode control for trajectory tracking and load sway rejection in double-pendulum overhead cranes," *IEEE Access*, vol. 7, pp. 10353–10361, 2019.

[5] S. Ding, J. H. Park, and C.-C. Chen, "Second-order sliding mode controller design with output constraint," *Automatica*, vol. 112, Feb. 2020, Art. no. 108704.

[6] L. Liu, W. X. Zheng, and S. Ding, "An adaptive SOSM controller design by using a sliding-mode-based filter and its application to buck converter," *IEEE Trans. Circuits Syst. I, Reg. Papers*, vol. 67, no. 7, pp. 2409–2418, Jul. 2020, doi: 10.1109/TCSI.2020.2973254.

[7] S. Ding and S. Li, "Second-order sliding mode controller design subject to mismatched term," *Automatica*, vol. 77, pp. 388–392, Mar. 2017.

[8] X.-H. Chang, J. Xiong, and J. H. Park, "Estimation for a class of parameter-controlled tunnel diode circuits," *IEEE Trans. Syst., Man, Cybern. Syst.*, early access, Aug. 13, 2018, doi: 10.1109/TSMC.2018.2859933.

[9] S. Yu, X. Yu, B. Shirinzadeh, and Z. Man, "Continuous finite-time control for robotic manipulators with terminal sliding mode," *Automatica*, vol. 41, no. 11, pp. 1957–1964, Nov. 2005.

[10] X. Liang, S. Li, and J. Fei, "Adaptive fuzzy global fast terminal sliding mode control for microgyroscope system," *IEEE Access*, vol. 4, pp. 9681–9688, 2016.

[11] H. Pan, G. Zhang, H. Ouyang, and L. Mei, "A novel global fast terminal sliding mode control scheme for second-order systems," *IEEE Access*, vol. 8, pp. 22758–22769, 2020.

[12] C. Xiu and P. Guo, "Global terminal sliding mode control with the quick reaching law and its application," *IEEE Access*, vol. 6, pp. 49793–49800, 2018.

[13] Y. Feng, X. H. Yu, and F. L. Han, "On nonsingular terminal sliding-mode control of nonlinear systems," *Automatica*, vol. 49, no. 6, pp. 1715–1722, Jun. 2013.

[14] J. Song, S. Song, and H. Zhou, "Adaptive nonsingular fast terminal sliding mode guidance law with impact angle constraints," *Int. J. Control, Autom. Syst.*, vol. 14, no. 1, pp. 99–114, Feb. 2016.

[15] Y. Wang, K. Zhu, F. Yan, and B. Chen, "Adaptive super-twisting nonsingular fast terminal sliding mode control for cable-driven manipulators using time-delay estimation," *Adv. Eng. Softw.*, vol. 128, pp. 113–124, Feb. 2019.

[16] A. Polyakov, "Nonlinear feedback design for fixed-time stabilization of linear control systems," *IEEE Trans. Autom. Control*, vol. 57, no. 8, pp. 2106–2110, Aug. 2012.

[17] J. Ni, L. Liu, C. Liu, X. Hu, and S. Li, "Fast fixed-time nonsingular terminal sliding mode control and its application to chaos suppression in power system," *IEEE Trans. Circuits Syst. II, Exp. Briefs*, vol. 64, no. 2, pp. 151–155, Feb. 2017.

[18] Y. Huang and Y. Jia, "Fixed-time consensus tracking control for second-order multi-agent systems with bounded input uncertainties via NFFTSM," *IET Control Theory Appl.*, vol. 11, no. 16, pp. 2900–2909, Nov. 2017.

[19] Y. Zhang, S. Tang, and J. Guo, "Adaptive terminal angle constraint interception against maneuvering targets with fast fixed-time convergence," *Int. J. Robust Nonlinear Control*, vol. 28, no. 1, pp. 2996–3014, Mar. 2018.

[20] M. L. Corradini and A. Cristofaro, "Nonsingular terminal sliding-mode control of nonlinear planar systems with global fixed-time stability guarantees," *Automatica*, vol. 95, pp. 561–565, Sep. 2018.

[21] B. Jiang, Q. Hu, and M. I. Friswell, "Fixed-time attitude control for rigid spacecraft with actuator saturation and faults," *IEEE Trans. Control Syst. Technol.*, vol. 24, no. 5, pp. 1892–1898, Sep. 2016.

[22] Q. Chen, S. Xie, M. Sun, and X. He, "Adaptive nonsingular fixed-time attitude stabilization of uncertain spacecraft," *IEEE Trans. Aerosp. Electron. Syst.*, vol. 54, no. 6, pp. 2937–2950, Dec. 2018.

[23] J. Gao, S. Zhang, and Z. Fu, "Fixed-time attitude tracking control for rigid spacecraft with actuator misalignments and faults," *IEEE Access*, vol. 7, pp. 15696–15705, 2019.

[24] Y. Tian, Y. Cai, and Y. Deng, "A fast nonsingular terminal sliding mode control method for nonlinear systems with fixed-time stability guarantees," *IEEE Access*, vol. 8, pp. 60444–60454, 2020.

[25] X.-H. Chang and G.-H. Yang, "A descriptor representation approach to observer-based H_∞ control synthesis for discrete-time fuzzy systems," *Fuzzy Sets Syst.*, vol. 185, no. 1, pp. 38–51, 2011.

[26] W.-H. Chen, J. Yang, L. Guo, and S. Li, "Disturbance-observer-based control and related methods—An overview," *IEEE Trans. Ind. Electron.*, vol. 63, no. 2, pp. 1083–1095, Feb. 2016.

[27] S. Ding, W.-H. Chen, K. Mei, and D. J. Murray-Smith, "Disturbance observer design for nonlinear systems represented by input–output models," *IEEE Trans. Ind. Electron.*, vol. 67, no. 2, pp. 1222–1232, Feb. 2020.

[28] M. Chen, Q.-X. Wu, and R.-X. Cui, "Terminal sliding mode tracking control for a class of SISO uncertain nonlinear systems," *ISA Trans.*, vol. 52, no. 2, pp. 198–206, Mar. 2013.

[29] J. Yang, S. Li, J. Su, and X. Yu, "Continuous nonsingular terminal sliding mode control for systems with mismatched disturbances," *Automatica*, vol. 49, no. 7, pp. 2287–2291, Jul. 2013.

[30] J. Su, J. Yang, and S. Li, "Continuous finite-time anti-disturbance control for a class of uncertain nonlinear systems," *Trans. Inst. Meas. Control*, vol. 36, no. 3, pp. 300–311, May 2014.

[31] S. Li, H. Sun, J. Yang, and X. Yu, "Continuous finite-time output regulation for disturbed systems under mismatching condition," *IEEE Trans. Autom. Control*, vol. 60, no. 1, pp. 277–282, Jan. 2015.

[32] L. Zhou, Z. Che, and C. Yang, "Disturbance observer-based integral sliding mode control for singularly perturbed systems with mismatched disturbances," *IEEE Access*, vol. 6, pp. 9854–9861, 2018.

[33] Q. Wang, H. Yu, M. Wang, and X. Qi, "An improved sliding mode control using disturbance torque observer for permanent magnet synchronous motor," *IEEE Access*, vol. 7, pp. 36691–36701, 2019.

[34] L. Tao, Q. Chen, and Y. Nan, "Disturbance-observer based adaptive control for second-order nonlinear systems using chattering-free reaching law," *Int. J. Control, Autom. Syst.*, vol. 17, no. 2, pp. 356–369, Jan. 2019.

[35] S. P. Bhat and D. S. Bernstein, "Finite-time stability of continuous autonomous systems," *SIAM J. Control Optim.*, vol. 38, no. 3, pp. 751–766, Jan. 2000.

[36] Z. Zuo, "Non-singular fixed-time terminal sliding mode control of non-linear systems," *IET Control Theory Appl.*, vol. 9, no. 4, pp. 545–552, Feb. 2015.
[37] L. Wang, T. Chai, and L. Zhai, "Neural-network-based terminal sliding-mode control of robotic manipulators including actuator dynamics," *IEEE Trans. Ind. Electron.*, vol. 56, no. 9, pp. 3296–3304, Sep. 2009.
[38] C. Edwards and Y. B. Shtessel, "Adaptive continuous higher order sliding mode control," *Automatica*, vol. 65, pp. 183–190, Mar. 2016.
[39] L. Yang and J. Yang, "Nonsingular fast terminal sliding-mode control for nonlinear dynamical systems," *Int. J. Robust Nonlinear Control*, vol. 21, no. 16, pp. 1865–1879, Nov. 2011.

HUIHUI PAN received the B.Eng. degree from the Nanjing Institute of Technology, Nanjing, China, in 2010, and the M. Eng. degree from the Shanghai University of Electric Power, Shanghai, China, in 2013. She is currently pursuing the Ph.D. degree with Nanjing Tech University, Nanjing. Since 2014, she has been with the College of Electrical Engineering, Tongling University, Tongling, China. Her major research interest includes sliding mode control and its application.

GUANGMING ZHANG received the B.Eng. degree from Nanjing Tech University, Nanjing, China, in 1988, and the M.Eng. and Ph.D. degrees from the PLA University of Science and Technology, in 1998 and 2002, respectively. Since 1998, he has been with the College of Electrical Engineering and Control Science, Nanjing Tech University, where he is currently a Professor. He has published more than 80 papers in journals and international conferences. His major research interest includes advanced control theory for mechatronics.

HUIMIN OUYANG (Member, IEEE) received the B.Eng. degree from the Tianjin Institute of Urban Construction, Tianjin, China, in 2005, the M.Eng. degree from the Nagoya Institute of Technology, Nagoya, Japan, in 2009, and the Ph.D. degree from the Toyohashi University of Technology, Toyohashi, Japan, in 2012. Since 2013, he has been with the College of Electrical Engineering and Control Science, Nanjing Tech University, Nanjing, China, where he is currently an Assistant Professor. He has published more than 30 papers in journals and international conferences. His research interest includes the system control theory and its application to mechatronics.

LEI MEI (Member, IEEE) received the B.Eng. degree from the Jiangsu University of Science and Technology, Zhenjiang, China, in 2000, the Ph.D. degree from the Nanjing University of Aeronautics and Astronautics, in 2009. Since 2009, he has been with the College Electrical Engineering and Control Science, Nanjing Tech University, Nanjing, China, where he is currently an Associate Professor. He has published more than 20 papers in journals and international conferences. His major research interests include motor design and flywheel energy storage technology and application.